doi:10.1016/j.jmb.2005.08.018 J. Mol. Biol. (2005) 353, 80–87

JMB

Available online at www.sciencedirect.com

SCIENCE DIRECT®

ELSEVIER

pH-Dependent Structural Changes at Ca^{2+}-binding Sites of Coagulation Factor IX-binding Protein

Nobuhiro Suzuki[1,2], Zui Fujimoto[1], Takashi Morita[3], Akiyoshi Fukamizu[2] and Hiroshi Mizuno[1,4,5]*

[1]*Department of Biochemistry National Institute of Agrobiological Sciences Tsukuba, Ibaraki 305-8602 Japan*

[2]*Institute of Applied Biochemistry, University of Tsukuba, Tsukuba, Ibaraki 305-8572, Japan*

[3]*Department of Biochemistry Meiji Pharmaceutical University, Kiyose, Tokyo 204-8588, Japan*

[4]*VALWAY Technology Center NEC Soft, Ltd., Koto-ku, Tokyo 136-8627, Japan*

[5]*Institute for Biological Resources and Functions National Institute of Advanced Industrial Science and Technology, Central 6, Tsukuba Ibaraki 305-8566, Japan*

**Corresponding author*

Coagulation factor IX-binding protein, isolated from *Trimeresurus flavoviridis* (IX-bp), is a C-type lectin-like protein. It is an anticoagulant consisting of homologous subunits, A and B. Each subunit has a Ca^{2+}-binding site with a unique affinity (K_d values of 14 μM and 130 μM at pH 7.5). These binding characteristics are pH-dependent and, under acidic conditions, the Ca^{2+} binding of the low-affinity site was reduced considerably. In order to identify which site has high affinity and to investigate the pH-dependent Ca^{2+} release mechanism, we have determined the crystal structures of IX-bp at pH 6.5 and pH 4.6 (apo form), and compared the Ca^{2+}-binding sites with each other and with those of the solved structures under alkaline conditions; pH 7.8 and pH 8.0 (complexed form). At pH 6.5, Glu43 in the Ca^{2+}-binding site of subunit A displayed two conformations. One (minor) is that in the alkaline state, and the other (major) is that at pH 4.6. However, the corresponding Gln43 residue of subunit B is in only a single conformation, which is almost identical with that in the alkaline state. At pH 4.6, Glu43 of subunit A adopts a conformation similar to that of the major conformer observed at pH 6.5, while Gln43 of subunit B assumes a new conformation, and both Ca^{2+} positions are occupied by water molecules. These results showed that Glu43 of subunit A is much more sensitive to protonation than Gln43 of subunit B, and the conformational change of Glu43 occurs around pH 6.5, which may correspond to the step of Ca^{2+} release.

© 2005 Elsevier Ltd. All rights reserved.

Keywords: C-type lectin-like protein; calcium binding; pH-dependent; crystal structure; snake venom

Introduction

Coagulation factor IX-binding protein (IX-bp), from the venom of the habu snake (*Trimeresurus flavoviridis*), belongs to a family of C-type lectin-like proteins (CLPs).[1] The crystal structure of IX-bp revealed a disulfide-linked heterodimer of C-type lectin-like subunits A (129 residues, 16.8 kDa) and B (123 residues, 15.7 kDa), with a unique 3D domain-swapping loop in the molecule.[2] It is very similar to the structures of other coagulation factor-binding proteins: factor IX/X-binding protein (IX/X-bp) from the venom of *T. flavoviridis*,[3] and factor X-binding protein (X-bp) from the venom of *Deinagkistrodon acutus*.[4] These proteins bind to γ-carboxyglutamic acid (Gla) domains of coagulation factors IX and X in the presence of Ca,$^{2+}$ thus blocking the amplification of the coagulation cascade[5–7] and, therefore, these proteins function as anticoagulants. Snake venom CLPs include, coagulation factor-binding proteins and proteins that bind to receptors of platelet and von Willebrand factors. The former proteins possess two Ca^{2+}-binding sites, except for the factor IX/X-binding protein from the venom of *Echis carinatus leucogaster*, which has one Ca^{2+}-binding site within subunit A.[8] On the other hand, the latter proteins have no Ca^{2+}-binding sites except for botrocetin, which has one metal-binding site within subunit B.[9]

Abbreviations used: IX-bp, coagulation factor IX-binding protein; IX/X-bp, coagulation factor IX/factor X-binding protein; X-bp, coagulation factor X-binding protein; CLP, C-type lectin-like protein; Gla, γ-carboxyglutamic acid; Mes, 2-(*N*-morpholino) ethanesulfonic acid.

E-mail address of the corresponding author: mizuno-hiroshi@aist.go.jp

0022-2836/$ - see front matter © 2005 Elsevier Ltd. All rights reserved.

Ca^{2+}-binding studies of the anticoagulant proteins IX-bp, IX/X-bp, and X-bp revealed that they have two independent Ca^{2+}-binding sites; a high-affinity site and a low-affinity site.[6–8,10] The crystal structures of IX-bp,[2] IX/X-bp[3] and the X-bp/Gla domain complex[4] showed that each subunit has one Ca^{2+}-binding site. The two Ca^{2+}-binding sites are formed by homologous and conserved residues: Ser41, Glu43, Glu47 and Glu128 in subunit A, and Ser41, Gln43, Glu47 and Glu120 in subunit B. Thus, the only difference exists at residue 43, suggesting that it could be responsible for the difference in the Ca^{2+}-binding affinity between subunits A and B. In the case of IX/X-bp, we found that the affinity of these binding sites, especially that of the low-affinity site, is pH-dependent, since the Ca^{2+} binding of the low-affinity site was reduced drastically as the pH value was decreased from 7.5 to 6.5, whereas that of the other was affected only slightly.[10] However, it is still not known which binding site has high or low affinity. Furthermore, the significance of Ca^{2+} binding to these sites is unclear. To address these questions, we at first revisited the Ca^{2+}-binding properties of IX-bp to examine the consistency of its pH-dependent Ca^{2+}-binding characteristics with those of IX/X-bp. We then conducted X-ray crystallographic analyses of habu IX-bp at different pH values to compare these structures with those obtained under different pH conditions. Furthermore, based on these comparisons of the structures around the Ca^{2+}-binding sites at different pH values, we investigated the pH-dependent Ca^{2+}-release mechanism of IX-bp.

Results

Description of the final models

Two crystal structures of IX-bp have been determined, at pH 6.5 and at pH 4.6 as the apo form. The crystals at pH 6.5 belong to the monoclinic space group $P2_1$, and the asymmetric unit contains two IX-bp molecules. The structure at pH 6.5 was determined at 1.72 Å resolution by the molecular replacement method, using the coordinates of the previously determined IX-bp structure at pH 7.8 (PDB code 1bj3).[2] The model contains 504 residues, four calcium ions, two polyethylene glycol 400 (PEG400) molecules and 568 water molecules. The crystallographic R-factor is 19.1% and R_{free} is 22.2%. The two molecules within the asymmetric unit are essentially very similar to each other, with a root-mean-square deviation (rmsd) of 0.51 Å, except in the flexible loop region in subunit A, where the conformation is slightly different due to intermolecular contacts.

The crystals of the apo form of IX-bp, on the other hand, belong to the monoclinic space group $C2$, and the asymmetric unit contains one heterodimer. The structure was refined at 2.29 Å resolution, and includes 252 residues, a chloride ion, two rubidium ions, a sulfate ion and 323 water molecules. The crystallographic R-factor is 21.2% and R_{free} is 21.4%. The refinement statistics for both structures are summarized in Table 1.

Table 1. Structure refinement statistics

	IX-bp at pH 6.5	Apo IX-bp at pH 4.6
Space group	$P2_1$	$C2$
Cell parameters		
a (Å)	60.72	134.12
b (Å)	63.51	37.83
c (Å)	66.91	55.83
ß (deg.)	117.01	110.46
Resolution (Å)	33.26–1.72	34.68–2.29
No. reflections in refinement	47,807	11,542
Completeness (%)	99.0	96.1
R_{work} (%)	19.1	21.2
R_{free} (%)	22.2	21.4
All non-hydrogen atoms	4692	2378
Protein non-hydrogen atoms	4094	2047
No. water molecules	568	323
No. calcium ions	4	0
No. PEG200 molecules	2	0
No. chloride ions	0	1
No. rubidium ions	0	2
No. sulfate ions	0	1
B-*factors*		
Average (Å^2)	17.8	32.1
Protein atoms (Å^2)	16.3	30.2
Water molecules (Å^2)	26.8	34.6
rmsd from ideal		
Bond lengths (Å)	0.005	0.006
Bond angles (deg.)	1.2	1.3
Dihedral angles (deg.)	22.8	22.7
Improper angles (deg.)	0.69	0.73

R_{free}-factors were calculated using 5% of the unique reflections.

The overall folds of these two structures are almost identical with each other and with those of IX-bp at pH 7.8 and IX-bp in complex with the Gla-domain of bovine factor IX at pH 8.0,[11] with rmsd of less than 1.0 Å for each pair (Figure 1). The differences in the backbone structures are observed in the flexible loop (A59–A63), a hinge region in subunit A (A73–A76) and the extended swapped loops (A80–A84 and B82–B85).

Ca^{2+}-binding sites

In the $F_o - F_c$ omit maps at pH 6.5, clear peaks are observed in the locations corresponding to the two calcium ions in the structure at pH 7.8.[2] These peaks were refined as calcium ions, since the peaks are significantly larger than those of the well-identified solvent molecules, and the average distances from the surrounding oxygen atoms are in the range of typical Ca^{2+}-binding distance (2.48 Å). The temperature factor of the Ca^{2+} in subunit A (Ca^{2+}-A) is 19.7 Å^2, which is greater than that of the Ca^{2+} in subunit B (Ca^{2+}-B), 14.2 Å^2, in contrast to the situation under alkaline conditions, where the temperature factor of Ca^{2+}-B is greater than that of Ca^{2+}-A.[2,11]

The coordination geometry at the Ca^{2+}-binding site in subunit B at pH 6.5 is identical with that at pH 7.8[2] and with that of the complex form at

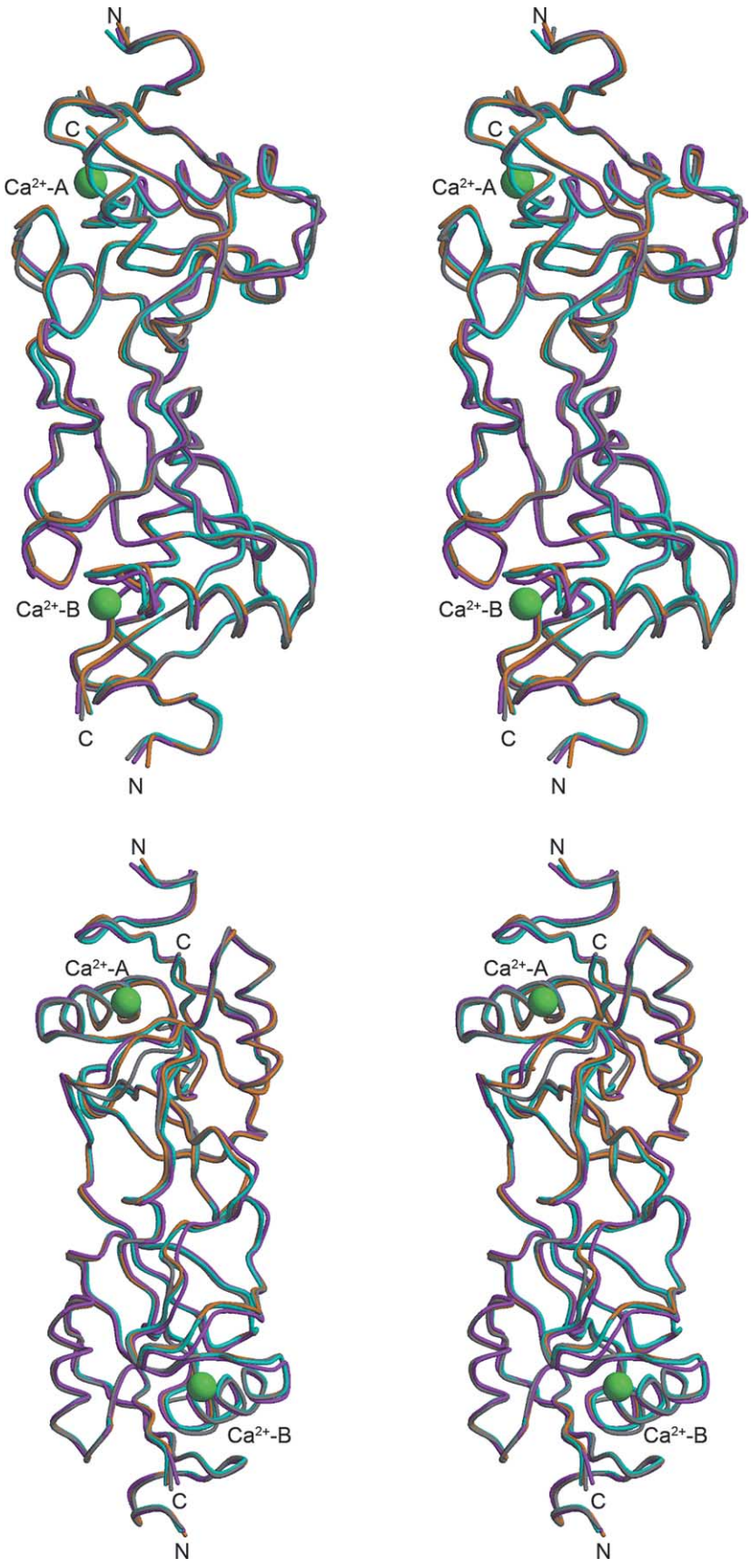

Figure 1. Stereoviews of the C^{α}-superimposed models of IX-bp at different pH values and different viewing angles (top and bottom). The models at pH 8.0, pH 7.8, pH 6.5 and pH 4.6 are shown in cyan, grey, orange and magenta, respectively. Calcium ions are drawn as green spheres.

pH 8.0,[11] a distorted pentagonal bipyramid, formed by the two oxygen atoms of SerB41, the $O^{\epsilon 1}$ atoms of GlnB43, GluB47 and GluB120, and two oxygen atoms from two water molecules, Wat4 and Wat5 (Figure 2(b)). On the other hand, the situation is slightly different in subunit A (Figure 2(a)). The two oxygen atoms of SerA41 and the $O^{\epsilon 1}$ atoms of GluA47 and GluA128 assume positions similar to those at pH 7.8,[2] and at pH 8.0.[11] However, one of the two water molecules (Wat1 and Wat2) present in the structure obtained under alkaline conditions is absent (Wat2). Furthermore, GluA43 adopts two conformations with partial occupancies. The minor portion (27%) of the side-chain of GluA43 binds to the Ca^{2+}-A through the $O^{\epsilon 2}$ atom in a manner similar to that in the structure obtained under alkaline conditions[2,11] (conformation I), while the majority of the remaining portion (64% occupancy) assumes a different conformation (conformation II), where the side-chain rotates by $\sim 30°$ around the χ-2 bond relative to conformation I. This conformational difference suggests a conformational change corresponding to an intermediate step that leads to the dissociation of the calcium ion (Figure 3(a)).

In the structure at pH 4.6, the peaks at the locations corresponding to the calcium ions are apparently too small to be refined as calcium ions, but have sizes similar to that of the solvent molecules. Therefore, these peaks were refined as water molecules in place of Ca^{2+}-A and Ca^{2+}-B, and are designated as Wat3 and Wat6, respectively. Wat3 is surrounded by only four oxygen atoms; two are from the carbonyl and side-chain oxygen atoms of SerA41, and the others are from the side-chain oxygen atoms of GluA47 and GluA128, as shown in Figure 2(a), forming hydrogen bonds with an average distance of 2.66 Å. GluA43 assumes conformation II (Figure 3(a)) and, as a result, the side-chain oxygen atom moves away from Wat3 (3.2 Å), and is slightly further away than the hydrogen bonding distance. On the other hand, Wat6 is surrounded by five oxygen atoms: backbone and side-chain oxygen atoms of SerB41, the $O^{\epsilon 1}$ atoms of GluB47 and GluB120, and a water molecule (Wat4), forming hydrogen bonds with an average distance

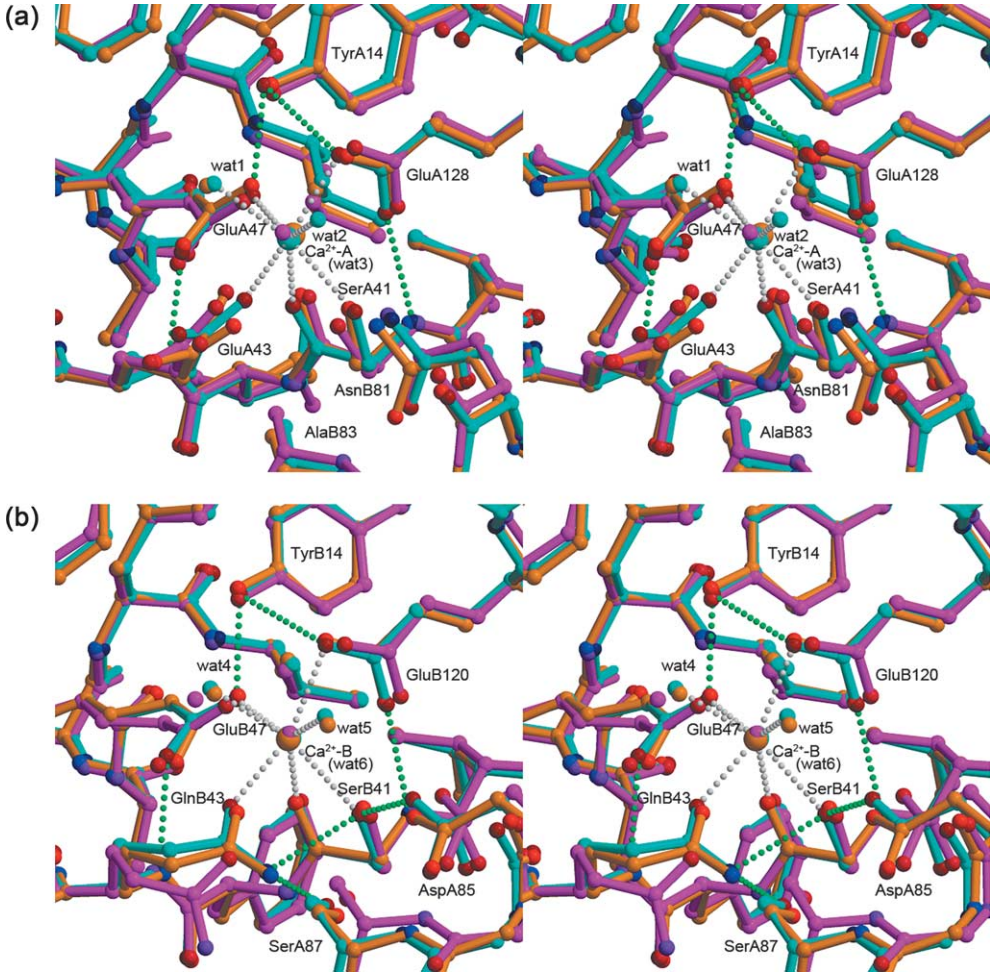

Figure 2. Stereoviews of ball-and stick models of the Ca^{2+}-binding sites of (a) subunit A and (b) subunit B. The models at pH 8.0, pH 6.5 and pH 4.6 are shown in cyan, orange and magenta, respectively. Dotted lines in grey and green indicate Ca^{2+} coordination and hydrogen bonds, respectively.

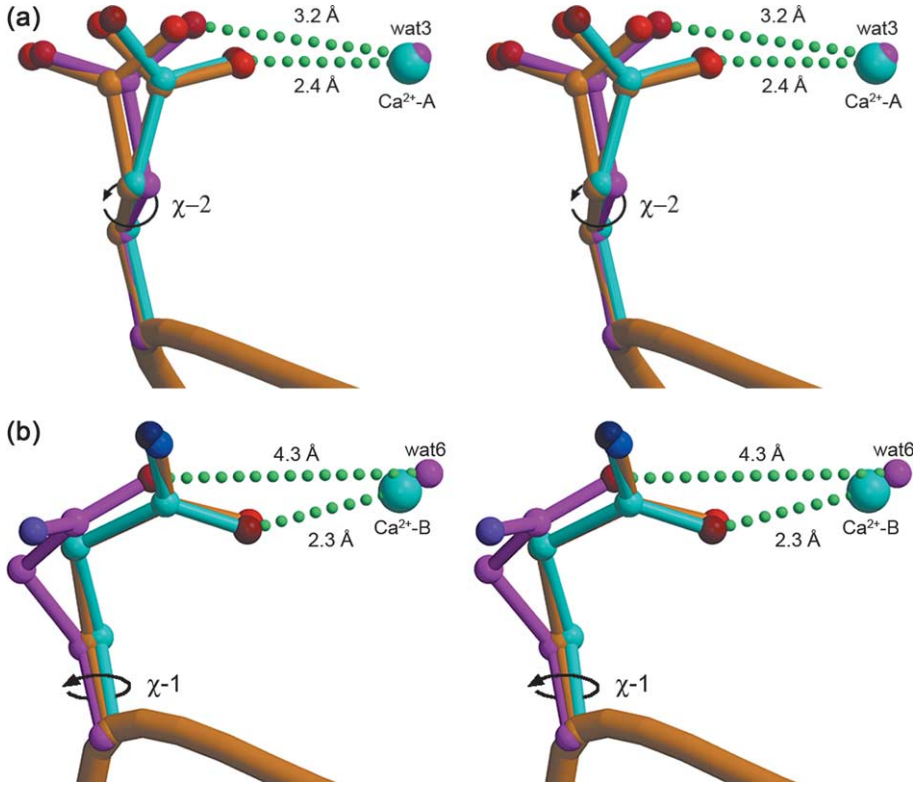

Figure 3. Close-up views of pH-dependent conformational changes of (a) GluA43 and (b) GlnB43 coordinating to the Ca^{2+}. Conformational changes are shown by the rotation of torsion angles. The models at pH 8.0, pH 6.5 and pH 4.6 are shown in cyan, orange and magenta, respectively.

of 2.73 Å (Figure 2(b)). The side-chain of GlnB43 adopts a different conformation, where the side-chain rotates by ~30° around the χ-1 bond, resulting in the increased distance between the peak center and the $O^{\epsilon 1}$ atom, as shown in Figure 3(b).

Fluorescence spectroscopy

The apparent Ca^{2+}-binding characteristics were investigated by the intrinsic tryptophan fluorescence technique. The K_d values are similar to our previous data for IX-bp,[6,8] IX/X-bp,[10] and X-bp.[7] The pH dependence of the lower-affinity binding is consistent with the data for IX/X-bp,[10] where the lower affinity dropped drastically when the pH value was lowered from 7.5 to 6.5, whereas the higher affinity decreased gradually.

Discussion

The Ca^{2+}-binding site in each subunit of IX-bp is identical with those of IX/X-bp,[3] the IX-bp/Gla domain complex,[11] and the X-bp/Gla domain complex.[4] Each binding site is composed of four conserved amino acid residues, forming a distorted pentagonal bipyramid configuration (Figure 2). A Ca^{2+}-binding assay using intrinsic tryptophan fluorescence measurements demonstrated that the Ca^{2+}-binding characteristics of IX-bp are similar to those of IX/X-bp,[10] as expected from the amino acid sequence similarity in the Ca^{2+}-binding sites (Table 2). Among the two independent Ca^{2+}-binding sites with different K_d values, the low-affinity Ca^{2+}-binding site has high pH-dependence (Table 2), and the Ca^{2+}-binding affinity decreases under acidic conditions, suggesting that these characteristics are common among these proteins.

The structure around the Ca^{2+}-A site at pH 6.5 is similar to that in the alkaline state, when GluA43 assumes conformation I, but it resembles that at pH 4.6 when GluA43 adopts conformation II. Therefore, the Ca^{2+}-A site is expected to be occupied by a calcium ion in the former structure, but by a water molecule (Wat3) in the latter structure. The peak

Table 2. Ca^{2+}-binding properties of habu IX-bp and habu IX/X-bp

	K_d values (μM)	
	High-affinity site	Low-affinity site
Previous work		
Habu IX/X-bp at pH 7.5[10]	25	200
Habu IX/X-bp at pH 6.5[10]	50	2000
Habu IX-bp at pH 7.5[6]	14	130
Habu IX-bp at pH 8.0[8]	16	109
Present work		
Habu IX-bp at pH 7.5	5	250
Habu IX-bp at pH 6.5	20	1700
Habu IX-bp at pH 4.6	48	3600

height at the Ca^{2+}-A site at pH 6.5 is thus reflected by a calcium ion and by a water molecule. Indeed, the Ca^{2+}-A and Ca^{2+}-B omit maps showed that the peak height of the Ca^{2+}-A site is considerably lower than that of the Ca^{2+}-B site, although it is not easy to estimate the precise occupancies of Ca^{2+} at both sites, because the occupancy and the temperature factor are closely correlated. Therefore it is reasonable that the temperature factor of Ca^{2+}-A is considerably higher than that of Ca^{2+}-B at pH 6.5, although that of Ca^{2+}-A is lower than that of Ca^{2+}-B at alkaline pH. These results suggest that the Ca^{2+}-A site is the low-affinity Ca^{2+}-binding site at pH 6.5. In Figure 3(a), the side-chain of GluA43 flips out of the Ca^{2+}-coordination sphere by rotating the χ-2 torsional angle, which results in its dissociation from the Ca^{2+}-A ion by increasing the distance from 2.4 Å to 3.2 Å. A similar observation was reported for pectate lyase C,[12] where one of the coordinated residues in the Ca^{2+}-binding site assumes two conformations with partial occupancies; one represents the Ca^{2+}-bound structure and the other represents the structure in the absence of Ca^{2+}. The other difference is the number of water molecules in the coordination sphere. In the structure obtained under alkaline conditions, two water molecules are bound to the Ca^{2+}, but one of them disappeared at pH 6.5 (Figure 2). As a consequence, the coordination number is reduced by 2, with a total of five oxygen atoms bound to the Ca^{2+} in subunit A. It was reported that the reduced coordination numbers negatively affect the Ca^{2+}-binding affinity in calmodulins,[13] and, hence, the Ca^{2+} affinity of the binding site in subunit A is likely to be lowered. Therefore, taking the aforementioned observations into account, it could alternatively be said that the crystal structure around the binding site in subunit A of IX-bp at pH 6.5 indicates that its Ca^{2+}-binding site is partially decalcified.

In contrast, there is no significant difference between the coordination geometries of subunit B under alkaline conditions and at pH 6.5, i.e. they both adopt a distorted pentagonal bipyramidal configuration, but this is clearly different from that of the Ca^{2+}-free state at pH 4.6. Therefore, it is quite likely that the binding site in subunit B is bound by a calcium ion with a higher occupancy at pH 6.5. Taking these observations into account, it can be deduced that the low Ca^{2+} affinity and the high pH-dependence are the characteristics of the binding site in subunit A.

Although the difference between the Ca^{2+}-binding characteristics of sites A and B is expected to be due to the difference between residue 43 at the Ca^{2+}-binding sites, i.e. GluA43 and GlnB43, the explanation is not so straightforward. In the case of calmodulin, a number of experiments have been conducted to investigate the effect of point mutations at the liganding residues of the Ca^{2+}-binding EF hands, which revealed that the mutation of an acidic residue to a neutral one (e.g. from Asp to Asn) can cause two contrary effects: it often reduces, but sometimes enhances, the Ca^{2+}-binding, probably due to the reduced repulsion among the coordinating group members.[14] In our case, as a portion of GluA43 moves away from the calcium ion by the rotation at χ-2 at pH 6.5, whereas no significant change occurs in the binding site in subunit B, the significance of GlnB43 appears to have the latter effect, so that the binding site in subunit B has the higher affinity for Ca^{2+}. In addition, Carrell *et al*. suggested another viewpoint, in which the *syn* conformation of the lone electron pair of the carboxyl oxygen atom displays a higher Ca^{2+}-binding affinity than the case of the *anti* conformation.[15] In this respect, the association between the Ca^{2+} and GluA43, which is coordinated to the Ca^{2+} in the *anti* conformation, is likely to be weaker than those of the other coordinating acidic residues, which are coordinated in the *syn* conformation. On the other hand, GlnB43 is coordinated to the Ca^{2+}-B in the *syn* conformation. This difference probably arises from the difference in their neighboring residues, AlaB83 and SerA87. In the B site, SerA87 binds to the $N^{\epsilon 2}$ atom of GlnB43, leading the $O^{\epsilon 1}$ atom to coordinate to the Ca^{2+}-B in the *syn* conformation. Furthermore, the effect of the lower pH is more serious with GluA43. When the pH level is lowered, changing the conditions from alkaline to acidic, the H^+ flux increases and some of the acidic residues of the protein become protonated, including the side-chain of GluA43, since it is highly exposed to the solvent. In the next place, the protonated GluA43 itself could dissociate from the Ca^{2+}, but a portion of the protonated GluA43 moves by a rotation at the χ-3 torsional angle, so that the protonated O^{ϵ} atom now faces the Ca^{2+}. Hence, the side-chain of GluA43 is repelled by the positive charge of the Ca^{2+}, and moves away by the rotation of the χ-2 torsional angle. Otherwise, the affinities of both binding sites are probably reduced gradually as the pH level decreases, since the other acidic side-chains in the coordination spheres can be protonated partially, due to their increased pK_a values including GluA43, as observed in calbindin D_{9k}.[16]

IX-bp binds to the Gla domain of factor IX through the concave surface, as revealed in the crystal structure of the IX-bp/Gla complex.[11] The binding affinity between IX/X-bp and the Gla domain reportedly decreased significantly at pH 6.5.[10] However, the concave surface is on the opposite side of the Ca^{2+}-binding sites (Figure 1(a)), and it exhibited no structural change, regardless of the pH changes. Therefore, it appears to be unlikely that Ca^{2+} is involved in this phenomenon. One of the possible reasons may simply be due to the surface potentials of the concave surface. We showed that various CLPs recognize distinct target molecules and bind them at their concave surfaces, in a surface potential-dependent manner.[17,18] Since the pH change also affects the concave surface potential, the affinity of IX-bp for the Gla domain may be reduced at a lower pH. On the other hand, the concentration of Ca^{2+}

also affects the affinity of IX/X-bp for the Gla domain.[10] The solution structure of the Ca^{2+}-free Gla domain of factor X revealed a striking difference between the Ca^{2+}-free and Ca^{2+}-bound forms. In the Ca^{2+}-free form, the Gla residues are exposed to the solvent, and Phe4, Leu5 and Val8 form a hydrophobic cluster in the interior of the domain.[19] The roles of the Ca^{2+} binding in IX-bp are not clear, but one of them should be to stabilize and to maintain the precise structure required for Gla domain binding.

Materials and Methods

Purification, crystallization and X-ray data collection

Habu IX-bp was purified by the standard procedure, from lyophilized venom of the habu snake.[6] Apo habu IX-bp was prepared by dialysis against a chelating resin-containing buffer.[6] The purified habu IX-bp was dialyzed at pH 6.5 (in 20 mM Mes buffer) and was crystallized by the microbatch method at 293 K. Rod-shaped crystals were obtained by mixing 0.5 μl of protein solution (6 mg ml^{-1}) and 1.5 μl of precipitant solution (20 mM Mes, 1 mM $CaCl_2$, 10% (w/v) PEG1000 and 10% (w/v) PEG8000). Apo habu IX-bp was crystallized by the sitting-drop, vapor-diffusion method at 293 K. Clusters of plate-like crystals were obtained by mixing 1 μl of protein solution (10 mg ml^{-1} in 20 mM sodium acetate buffer at pH 4.6) and an equal volume of precipitant solution (0.2 M ammonium sulfate, 0.1 M rubidium acetate (pH 4.6), and 30% (w/v) polyethylene glycol monomethylether) equilibrated against 50 μl of the precipitant solution. X-ray diffraction data of the habu IX-bp crystal at pH 6.5 and the apo habu IX-bp crystal were collected at 100 K, using R-axis IV^{++} and R-axis VII imaging plate detectors, respectively, and CuK_α radiation generated by Rigaku rotating-anode generators (Ultrax-18 and MicroMax007, respectively). Crystallization and data collection were done as described.[20]

Structure determination and refinement

Initial models of habu IX-bp at pH 6.5 and apo habu IX-bp were obtained by the molecular replacement method, with the program AMoRe[21] in the CCP4 program package,[22] using the coordinates from the previously solved crystal structure of habu IX-bp at pH 7.8 (PDB code 1bj3)[2] as a search model. The resultant models were first subjected to rigid-body refinement, followed by cycles of simulated annealing, energy minimization and individual *B*-factor refinement using CNS,[23] with visual inspection and manual modification of the models using QUANTA2000 (Accelrys) and XtalView.[24] When the *R* factors dropped to 0.25, the solvent molecules were added automatically by CNS and manually by QUANTA2000 and XtalView. Finally, the multiple conformations of GluA43 at pH 6.5 were refined with CNS and XtalView as follows. (1) The temperature factors of the double conformations of GluA43 were refined with fixed occupancies (both at 0.5), and then (2) the grouped occupancies of the double conformer were refined after averaging the temperature factors. (3) Further refinement of the temperature factors was conducted using the obtained occupancy. The final temperature factors of the individual atoms were refined after the temperature factors and the grouped occupancies were alternately refined until convergence. The final models were checked by PROCHECK[25] and WHATCHECK.[26] The refinement statistics are summarized in Table 1. Figures were drawn using the programs MOLSCRIPT[27] and Raster3D.[28]

Measurement of fluorescence intensity

Ca^{2+}-induced changes in the intrinsic fluorescence of habu IX-bp were measured using a Hitachi Fluorescence Spectrophotometer F4500 equipped with a thermostatically controlled cell-holder as described.[10] K_d values were estimated by curve-fitting by least-squares calculations.

Protein Data Bank accession number

The atomic coordinates of IX-bp at pH 6.5 and 4.6 (as the apo form) have been deposited in the RCSB Protein Data Bank, Research Collaboratory for Structural Bioinformatics, New Brunswick, NJ, through the Protein Data Bank Japan, Osaka University, under the code names 1X2T and 1X2W, respectively.

Acknowledgements

This research was supported by Science Research Grants-in-Aid (to T.M.) and by Special Coordination Funds for Promoting Science and Technology from the Ministry of Education, Science, Sports and Culture of Japan (to H.M.).

References

1. Atoda, H., Hyuga, M. & Morita, T. (1991). The primary structure of coagulation factor IX/factor X-binding protein isolated from the venom of *Trimeresurus flavoviridis*. Homology with asialoglycoprotein receptors, proteoglycan core protein, tetranectin, and lymphocyte Fc epsilon receptor for immunoglobulin E. *J. Biol. Chem.* **266**, 14903–14911.
2. Mizuno, H., Fujimoto, Z., Koizumi, M., Kano, H., Atoda, H. & Morita, T. (1999). Crystal structure of coagulation factor IX-binding protein from habu snake venom at 2.6 Å: implication of central loop swapping based on deletion in the linker region. *J. Mol. Biol.* **289**, 103–112.
3. Mizuno, H., Fujimoto, Z., Koizumi, M., Kano, H., Atoda, H. & Morita, T. (1997). Structure of coagulation factors IX/X-binding protein, a heterodimer of C-type lectin domains. *Nature Struct. Biol.* **4**, 438–441.
4. Mizuno, H., Fujimoto, Z., Atoda, H. & Morita, T. (2001). Crystal structure of an anticoagulant protein in complex with the Gla domain of factor X. *Proc. Natl Acad. Sci. USA*, **98**, 7230–7234.
5. Atoda, H. & Morita, T. (1989). A novel blood coagulation factor IX/factor X-binding protein with anticoagulant activity from the venom of *Trimeresurus flavoviridis* (Habu snake): isolation and characterization. *J. Biochem.* **106**, 808–813.
6. Atoda, H., Ishikawa, M., Yoshihara, E., Sekiya, F. & Morita, T. (1995). Blood coagulation factor IX-binding

protein from the venom of *Trimeresurus flavoviridis*: purification and characterization. *J. Biochem.* **118**, 965–973.
7. Atoda, H., Ishikawa, M., Mizuno, H. & Morita, T. (1998). Coagulation factor X-binding protein from *Deinagkistrodon acutus* venom is a Gla domain-binding protein. *Biochemistry*, **37**, 17361–17370.
8. Atoda, H., Kaneko, H., Mizuno, H. & Morita, T. (2002). Calcium-binding analysis and molecular modeling reveal echis coagulation factor IX/factor X-binding protein has the Ca-binding properties and Ca ion-independent folding of other C-type lectin-like proteins. *FEBS Letters*, **531**, 229–234.
9. Sen, U., Vasudevan, S., Subbarao, G., McClintock, R. A., Celikel, R., Ruggeri, Z. M. & Varughese, K. I. (2001). Crystal structure of the von Willebrand factor modulator botrocetin. *Biochemistry*, **40**, 345–352.
10. Sekiya, F., Yamashita, T. & Morita, T. (1995). Role of calcium(II) ions in the recognition of coagulation factors IX and X by IX/X-bp, an anticoagulant from snake venom. *Biochemistry*, **34**, 10043–10047.
11. Shikamoto, Y., Fujimoto, Z., Morita, T. & Mizuno, H. (2003). Crystal structure of Mg^{2+}- and Ca^{2+}-bound Gla domain of factor IX complexed with binding protein. *J. Biol. Chem.* **278**, 24090–24094.
12. Herron, S. R., Scavetta, R. D., Garrett, M., Legner, M. & Jurnak, F. (2003). Characterization and implications of Ca^{2+} binding to pectate lyase C. *J. Biol. Chem.* **278**, 12271–12277.
13. Maune, J. F., Klee, C. B. & Beckingham, K. (1992). Ca^{2+} binding and conformational change in two series of point mutations to the individual Ca^{2+}-binding sites of calmodulin. *J. Biol. Chem.* **267**, 5286–5295.
14. Waltersson, Y., Linse, S., Brodin, P. & Grundstrom, T. (1993). Mutational effects on the cooperativity of Ca^{2+} binding in calmodulin. *Biochemistry*, **32**, 7866–7871.
15. Carrell, C. J., Carrell, H. L., Erlebacher, J. & Glusker, J. P. (1988). Structural aspects of metal ion carboxylate interactions. *J. Am. Chem. Soc.* **110**, 8651–8656.
16. Kesvatera, T., Jonsson, B., Thulin, E. & Linse, S. (2001). Focusing of the electrostatic potential at EF-hands of calbindin D(9k): titration of acidic residues. *Proteins: Struct. Funct. Genet.* **45**, 129–135.
17. Hirotsu, S., Mizuno, H., Fukuda, K., Qi, M. C., Matsui, T., Hamako, J. *et al*. (2001). Crystal structure of bitiscetin, a von Willebrand factor-dependent platelet aggregation inducer. *Biochemistry*, **40**, 13592–13597.
18. Horii, K., Okuda, D., Morita, T. & Mizuno, H. (2003). Structural characterization of EMS16, an antagonist of collagen receptor (GPIa/IIa) from the venom of *Echis multisquamatus*. *Biochemistry*, **42**, 12497–12502.
19. Sunnerhagen, M., Forsen, S., Hoffren, A. M., Drakenberg, T., Teleman, O. & Stenflo, J. (1995). Structure of the Ca^{2+}-free Gla domain sheds light on membrane binding of blood coagulation proteins. *Nature Struct. Biol.* **2**, 504–509.
20. Suzuki, N., Shikamoto, Y., Fujimoto, Z., Morita, T. & Mizuno, H. (2005). Crystallization and preliminary X-ray analysis of coagulation factor IX-binding protein from habu snake venom at pH 6.5 and 4.6. *Acta Crystallog. sect. F*, **61**, 147–149.
21. Navaza, J. (1994). AMoRe: an automated package for molecular replacement. *Acta Crystallog. sect. A*, **50**, 157–163.
22. Collaborative Computational Project, Number 4. (1994). The CCP4 suite: programs for protein crystallography. *Acta Crystallog. sect. D*, **50**, 760–763.
23. Brünger, A. T., Adams, P. D., Clore, G. M., DeLano, W. L., Gros, P., Grosse-Kunstleve, R. W. *et al*. (1998). Crystallography & NMR system: a new software suite for macromolecular structure determination. *Acta Crystallog. sect. D*, **54**, 905–921.
24. McRee, D. E. (1999). XtalView/Xfit—a versatile program for manipulating atomic coordinates and electron density. *J. Struct. Biol.* **125**, 156–165.
25. Laskowski, R. A., MacArthur, M. W., Moss, D. S. & Thornton, J. M. (1993). PROCHECK: a program to check the stereochemical quality of protein structures. *J. Appl. Crystallog.* **26**, 283–291.
26. Hooft, R. W., Vriend, G., Sander, C. & Abola, E. E. (1996). Errors in protein structures. *Nature*, **381**, 272.
27. Kraulis, P. J. (1991). MOLSCRIPT: a program to produce both detailed and schematic plots of protein structures. *J. Appl. Crystallog.* **24**, 946–950.
28. Merritt, E. A. & Bacon, D. J. (1997). Raster3D: photorealistic molecular graphics. *Methods Enzymol.* **277**, 505–524.

Edited by R. Huber

(Received 17 May 2005; received in revised form 8 August 2005; accepted 11 August 2005)
Available online 31 August 2005